CRYSTAL GROWTH & DESIGN

Article

pubs.acs.org/crystal

Smaller Calcite Lattice Deformation Caused by Occluded Organic Material in Coccoliths than in Mollusk Shell

S. Frølich,[†] H. O. Sørensen,[‡] S. S. Hakim,[‡] F. Marin,[§] S. L. S. Stipp,[‡] and H. Birkedal*[,†]

[†]iNANO and Department of Chemistry, Aarhus University, 14 Gustav Wieds Vej, 8000 Aarhus, Denmark

[‡]Nano-Science Center, Department of Chemistry, University of Copenhagen, Universitetsparken 5, 2100 Copenhagen Ø, Denmark

[§]UMR CNRS 6282 Biogéosciences, Université de Bourgogne, 6 Boulevard Gabriel, Dijon, France

ABSTRACT: The growth and nucleation of biominerals are directed and affected by associated biological molecules. In this paper, we investigate the influence of occluded biomolecules on biogenic calcite from the coccolithophorid *Pleurochrysis carterae* and from chalk, a rock composed predominantly of fossil coccoliths. We compare the results with data on chalk from the extensively studied mussel *Pinna nobilis* that served as a control. Using high resolution synchrotron powder X-ray diffraction combined with *in situ* heating, the influence of organic compounds on the structure of the inorganic phase was probed. Two heating cycles allow us to differentiate the effects of thermal agitation and organic molecules. Single peak analysis and Rietveld refinement were combined to show significant differences resulting from the occluded biomolecules on the mineral phase in biogenic calcite in the mollusk shell and the coccolithophorids. These differences were reflected in lattice deformation (macrostrain), structure (microstrain), and atomic disorder distributions ($\delta_{organic}$). The influence of the biological macromolecules on the inorganic phase was consistently smaller in the *P. carterae* compared to *P. nobilis*. This suggests that the interaction between biomolecules and calcite is not as tight in the coccoliths as in the shell. Although the shape of chalk has been preserved over millions of years, no major influence on the crystal lattice was observed in the chalk samples.

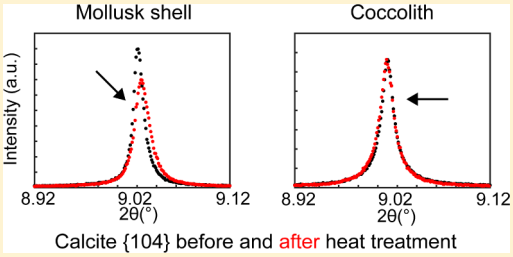

INTRODUCTION

Many organisms control the polymorph, size, morphology, and orientation of crystals in biominerals.[1,2] This high level of control is achieved in part through interaction between organic molecules and their inorganic counterparts. Inter- and intracrystalline biomolecules direct and control the nucleation and growth of the crystals.[3−5] A thorough understanding of the intimate interplay between organic phases and the growing mineral in these nanocomposite structures would help us understand the details of material design in nature, laying the foundation for the development of new composite "bioinspired" materials with fascinating properties.[6] The interplay between biological macromolecules and the inorganic mineral phases can be very intimate indeed. In mollusk shells, occluded biomacromolecules have been shown to lead to lattice deformation in both aragonite and calcite.[7−12] While the magnitude of the changes varies with mollusk species, the sign (compressive or expansive) of the deformation is the same.[9,10] In the calcified byssus of the bivalve *Anomia simplex*,[13−16] lattice deformation was also observed in aragonite, but the deformation had a different distribution of signs than in shells,[17] suggesting that there is no general pattern for lattice deformation.

The biomolecules interacting with minerals in nature can be roughly separated into two categories: polysaccharides (PSs) and proteins.[3,18] Many research groups have worked on elucidating the role of biomolecules in crystallization of biominerals by mainly focusing on proteins.[3,19,20] Although the association of PSs with biominerals has been realized for a long time,[21−24] more recently, their role in biomineralization has been emphasized.[25−30] Indeed, acidic PSs are the main components directing coccolith formation,[31,32] in contrast with the predominance of proteins for many other biominerals.[3,18] Coccolithophorids are unicellular marine phytoplankton. They grow a protective cage composed of coccoliths, which are shields of roughly 3 μm in diameter, made of 20−60 individual calcite single crystals (Figure 1). These crystals are arranged at highly specific positions with precise orientations, giving the coccoliths a complex, species-specific structure.

It is not known whether the interactions between the polysaccharides and the mineral are the same as for proteins. The polysaccharide, chitin, is well-known for its role in biomineralization, but it serves mainly as a structural component and does not support calcium carbonate nucleation.[27,33] In coccolithophorids such as *Pleurochrysis carterae*, which we use as the model coccoliths in this study, the PSs have been shown to protect the calcite against dissolution, as well as affect the growing mineral.[28,29,34−40] The coccoliths from *P. carterae* contain approximately the same proportion of organic material as observed in molluscan calcite.[5] In *P. carterae*, three PSs, denoted PS-1, PS-2, and PS-3, are essential for various parts of the mineralization process:

Received: January 27, 2015
Revised: March 18, 2015
Published: April 20, 2015

DOI: 10.1021/acs.cgd.5b00118
Cryst. Growth Des. 2015, 15, 2761−2767

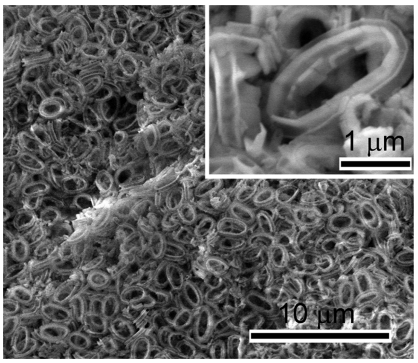

Figure 1. Scanning electron micrograph of *Pleurochrysis carterae* coccoliths, extracted from cultured material.

PS-1 and PS-2 bind calcium and deliver it to the growth site. PS-2 also plays a role in the creation of a protococcolith ring of calcite crystals, which acts as the base for the further formation of the coccolith shield, and PS-3 helps shape the coccolith.[31,36,37]

In this work, we compare the influence of occluded organic molecules in the biogenic calcite produced by the coccolithophorid *P. carterae*, with that of the mussel *Pinna nobilis* and that of chalk. In *P. nobilis*, mainly proteins are associated with the mineral,[41−43] in comparison with the PSs described in *P. carterae*. Chalk is composed predominantly of biogenic calcite in the form of fossilized coccoliths. There is often some recrystallization in chalk, but recognizable coccoliths and the coccospheres they create are common.[44] That the coccolith morphology is so well preserved over geologic time suggests that the material is stabilized. Indeed, biomolecules can be extracted from chalk, and these resemble fragments of the PS known from current coccolithophorids.[45] Such extracted molecules retain their ability to influence calcite crystallization kinetics *in vitro*,[28−30,46] demonstrating that PS retains its activity even after aging over many millions of years. In turn, this prompts the question of whether these molecules also maintain lattice deformation in coccoliths.

To address the questions about the impacts of PS in biomineralization, we investigated calcite of different origins, using high resolution synchrotron powder X-ray diffraction (PXRD). The occlusion of large biological molecules within the crystalline structure of a biomineral would intimately affect the crystal structure. By using the very bright and highly monochromatic X-rays of a synchrotron, even the smallest perturbations in the inorganic phase can be detected, providing the data needed for deciphering how the crystal structure is affected by the organic molecules. By performing two *in situ* heating experiments burning off the organic components, it is possible to separate the contributions to lattice strain that results from thermal expansion and from occluded biomolecules.[47] We examined the crystalline structure using Rietveld refinement and single peak fitting.

EXPERIMENTAL DETAILS

Samples. The *P. nobilis* shell was from a specimen recently collected off the marine biology station of Villefranche-sur-mer (Alpes Maritimes, France), in accordance with the DREAL PACA regulations. In the subsequent experiments, only the outer calcitic shell layer, made of "simple-type" prisms, was used as a shell reference. Coccoliths were obtained from culturing the species, *Pleurochrysis carterae*, CCMP645, acquired from the Provasoli-Guillard National Center for Culture of Marine Phytoplankton. We followed the procedure previously described[48] with slight modifications. The algae were grown in 2 L flasks at 17 °C under constant air bubbling and illumination in an F/2 medium that had been made with seawater collected at Helsingør, Denmark,[49,50] filtered and autoclaved. To prepare the sample, the algae were left for 2 weeks in air to die and sediment. The slurry was centrifuged at 8000*g* for 10 min, resuspended in seawater, and centrifuged once more. Six grams of sediment was resuspended in 1 L of 50 mM $NaHCO_3$ and sonicated for 2 min and then centrifuged again. The resuspension and centrifugation steps were repeated twice more. Finally, the pellet of coccoliths was washed with 50 mM $NaHCO_3$. We also examined two types of chalk: a fragment from a core drilled in a Maastrichtian formation in the North Sea Basin (C24) and a sample taken from a few meters below the ground surface in a Danian Formation, at Klintholm, Funen, Denmark. No trace of vaterite was observed in the XRD patterns, even though this may occur in seawater cultures as seen for *P. carterae* by Andersson et al.[48]

Synchrotron X-ray Powder Diffraction. Samples were ground in an agate mortar, placed in 0.3 mm diameter quartz capillaries, and mounted on a rotating stage for better grain averaging. Diffractograms were collected as a function of temperature in the following way: First cycle: room temperature (RT), 373, 473, 623 K, then cooling to room temperature and the second cycle: RT, 373, 473, 623 K. The diffraction data were collected at the high resolution diffractometer of ID31 of the ESRF, Grenoble, France, using X-rays with an energy of 26 keV (λ = 0.4768 Å). The data sets covered the 2θ range from 0 to 52.5° in 0.001° steps. The instrument line broadening was determined using a Si reference and included in the Rietveld refinements (fwhm for Si {111} = 0.0038°). For the single peak analysis, the observed instrument line broadening was significantly lower than the line broadening extracted from the fits. No traces of CaO were observed, indicating that no detectable $CaCO_3$ decomposition took place within the closed capillaries.

Peak Fitting. Individual peaks were analyzed using asymmetrical pseudo-Voigt fitting routines in MATLAB.[51] A linear background and the asymmetrical fit yielded very high quality fits, and the full width at half-maximum (fwhm) could be obtained. In general, line broadening in powder diffraction results from microstrain fluctuations, crystallite size, and instrument broadening.[52] With highly monochromatic synchrotron X-rays, the instrument contribution is effectively negligible, so the size of coherently scattering domains in the crystallites and the microstrain fluctuations in the lattice dominate line broadening. In the case of strain broadening, the fwhm can be related to the relative change in *d*-spacing through the following equation:[53]

$$\Delta 2\theta = \frac{\Delta d}{d} \tan(\theta)$$

The widths that we have reported from the individual peaks, as $\Delta d/d$, were calculated using this formula. Hence the reported values reflect a mixture of crystal size and strain broadening effects. We used this approach because the chance that there is a distribution of size broadening and/or strain broadening effects precludes the possibility of separating the effects by single peak fitting.

Rietveld Refinement. Rietveld refinement was carried out in the FullProf Software Suite[54] with a linear interpolation between points as background. For the *P. nobilis*, C24 and Klintholm samples, two distinct calcite phases were observed and incorporated into the refined model. For the chalk samples, two distinct phases are expected because the sample is a mixture of fossil biogenic calcite and calcite that has resulted from some degree of recrystallization. Recrystallized calcite could originate from coccoliths or from the remains of some other organism. For the material from the *P. nobilis* shell, different effects of the organic phase on the biomineral could be expected, as was suggested but not observed, by Pokroy et al.[7] For the C24 sample, KCl and aragonite impurities were included in the model.

Individual isotropic displacement parameters were used for all atoms, except in the C24 sample, where an overall displacement parameter was used. Where several calcite phases were present, the displacement parameters were constrained to the same value. In *P. carterae*, a two-term spherical harmonic size broadening term was included and in *P. nobilis*, a single parameter was used to describe the

DOI: 10.1021/acs.cgd.5b00118
Cryst. Growth Des. 2015, 15, 2761−2767

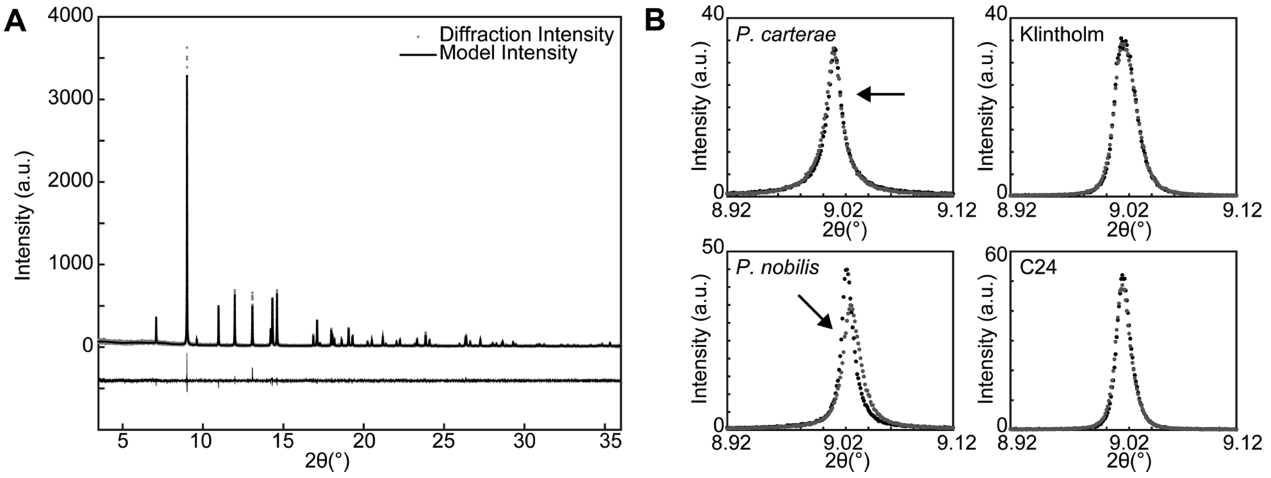

Figure 2. (A) Example diffractogram of calcite from *P. carterae* sample between cycles and (B) {104} Bragg peaks at room temperature before (black) and after (gray) the first heating for the four calcite samples. The arrows indicate the direction of movement of the peaks.

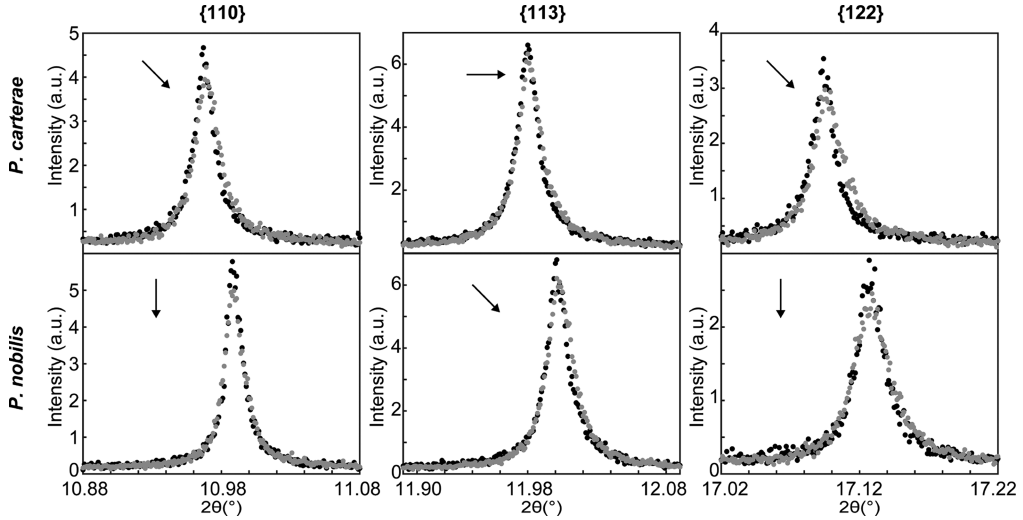

Figure 3. Bragg peaks {110}, {113}, and {122} plotted at room temperature before (black) and after (gray) the first heating for *P. carterae* and *P. nobilis*. The arrows indicate the direction of peak movement after heating.

preferred orientation induced by the needle-like shape of the shell prisms.

The lattice strain was estimated by subtraction of the effects of thermal expansion.[17] This was done by subtracting the lattice constant value from the second heating cycle from that of the first cycle and normalizing to excess macrostrain by dividing by the room temperature unit cell parameter. Hence for the *c*-axis at 300 K, $\varepsilon_{300} = (c_{300,1^{st}} - c_{300,2^{nd}})/c_{RT,2^{nd}} \cdot 100\%$.

RESULTS

Figure 2 shows high resolution synchrotron data collected on the two recent biological samples, the calcitic prisms of the large fan mussel *P. nobilis* and cultured coccoliths from the coccolithophorid *P. carterae*, as well as two chalk samples, collected from just below the surface at Klintholm on Funen in Denmark and from a core drilled in the North Sea Basin, here called C24. Figure 2A shows the diffractogram measured at room temperature with the accompanying Rietveld fit for *P. carterae* after the first heating round. The material is phase pure and adequately fitted by the Rietveld model. The applied heat treatment leads to significant changes for the freshly biomineralized samples. Figure 2B compares the room temperature diffraction data of the calcite {104} peak before and after heat treatment for the four samples. The peak in the *P. carterae* diffractogram shifts to a lower angle in contrast to *P. nobilis,* where a shift to a higher angle as well as peak broadening is observed. The *P. nobilis* behavior is in accordance with expectations.[7,9,11] The two chalk samples show the same trends: only an insignificant change in peak shape and position is seen.

In Figure 3, additional peaks from the diffractograms are plotted to explore the difference in behavior for calcite from *P. nobilis* and *P. carterae*. The differences in behavior indicate how the mineral is affected differently by the organic phase in the two samples. The data suggest that while there is significant change in the *c*-axis and minimal change in the *a*-axis for *P. nobilis*, a different picture is seen in *P. carterae*. The peaks {110} and {122} shift to higher angles. These peaks remain essentially unchanged in *P. nobilis*. Substitution of magnesium into the calcite lattice can affect the unit cell size and thereby the position of the peaks. However, the effect of substitution will not be affected by the heat treatment that is below diffuse onset temperatures;[8] the observed changes thus result from other effects.

DOI: 10.1021/acs.cgd.5b00118
Cryst. Growth Des. 2015, 15, 2761−2767

Quantitative insights into the heat-induced changes were obtained by single peak fitting, which gave the fwhm of the peaks. Figure 4 compares the peak widths for selected

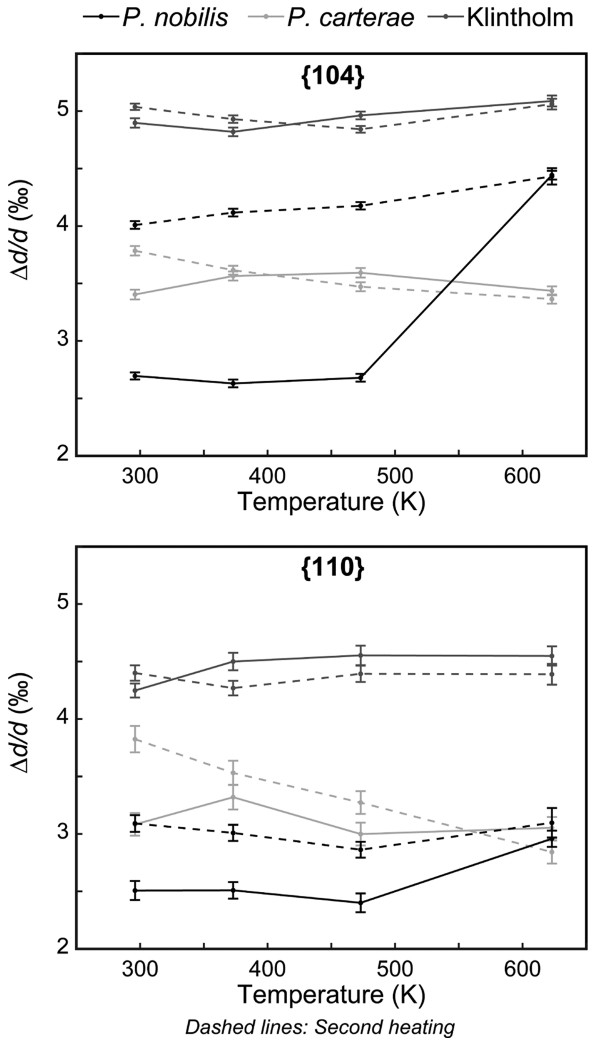

Figure 4. $\Delta d/d$ obtained from asymmetric pseudo-Voigt fits, as a function of temperature, for the {104} and {110} reflections for *P. nobilis* (black), *P. carterae* (light gray), and Klintholm (dark gray). The first heat cycle is plotted with solid lines, the second, with dashed lines. In some cases, error bars are smaller than the size of the symbol. C24 data are not shown because they follow the same trend as the Klintholm data.

reflections, expressed as effective $\Delta d/d$. For the Klintholm sample, $\Delta d/d$ is high and largely insensitive to heating for both the {104} and {110} peaks. The large value indicates a distribution of unit cell parameters that is consistent with the partial recrystallization observed, whereas the insensitivity to heating indicates minimal influence of organic biomolecules on the atomic mineral structure.

The chalk sample has higher values of $\Delta d/d$ compared to calcite from mussel and algae. For the shell of *P. nobilis*, heating produced a large difference in $\Delta d/d$ for reflections with a component along the *c*-axis (only {104} shown). During the first heating cycle, a large increase in $\Delta d/d$ was seen for temperatures above 600 K, whereas for the second heating, only a small change with temperature was observed. These differences are attributed to the buildup of local lattice fluctuations as a result of the loss of organic molecules.[7] A similar behavior was seen for reflections without components along the *c*-axis, although with a less pronounced difference between first and second cooling. In contrast, for *P. carterae*, there was negligible difference for the {104} peak between first and second heating, whereas for the {110} reflection, $\Delta d/d$ changed between the two cycles. The dissimilar behavior for the *P. carterae* and *P. nobilis* samples suggests that the mineral and the organic phase interact differently in the two samples.

Full Rietveld refinement was performed on each of the diffraction patterns, as exemplified by the fit shown in Figure 1A. The refined unit cell parameters for all temperatures are reported in Table 1. The unit cell parameters for *P. nobilis* agree

Table 1. Unit Cell *a*- and *c*-Axis Parameters in Å at Room Temperature, Obtained from Rietveld Refinement

		a-axis (Å)		
		first heating	second heating	difference
P. carterae		4.99066(1)	4.98953(2)	−0.00113(2)
P. nobilis	Phase 1	4.98091(2)	4.98116(3)	0.00025(4)
	Phase 2	4.9784(1)	4.97938(7)	0.0009(1)
Klintholm	Phase 1	4.98878(2)	4.98798(2)	−0.00080(3)
	Phase 2	4.98201(4)	4.98162(5)	−0.00040(6)
C24	Phase 1	4.98838(2)	4.98812(2)	−0.00026(3)
	Phase 2	4.98674(3)	4.98633(3)	−0.00040(4)
		c-axis (Å)		
		first heating	second heating	difference
P. carterae		17.06342(7)	17.06845(8)	0.0050(1)
P. nobilis	Phase 1	17.0534(1)	17.0462(2)	−0.0072(3)
	Phase 2	17.0431(4)	17.0279(3)	−0.0152(5)
Klintholm	Phase 1	17.0579(1)	17.0596(1)	0.0017(1)
	Phase 2	17.0261(2)	17.0251(2)	−0.0010(3)
C24	Phase 1	17.05862(8)	17.0614(1)	0.0027(1)
	Phase 2	17.0483(1)	17.0548(1)	0.0065(2)

well with the values, a = 4.98138(2) Å and c = 17.05803(9) Å previously reported by Pokroy et al.[9] The small differences can be ascribed to biological variation between specimens and minor differences in the instrument. The high degree of agreement between these two independent determinations of unit cell parameters for *P. nobilis* indicate similar levels of magnesium in the sample we investigated and that investigated by Pokroy et al.[9] Considering the known relation between the calcite unit cell parameters and magnesium content[55] and taking into account the precision of our measurements and the known magnesium content in *P. nobilis*, we conclude that there is only an insignificant amount of magnesium in *P. carterae*.

In the chalk samples, smaller differences were observed than for the fresh samples. For the modern samples, the temperature influence on macrostrain is shown in Figure 5. The temperature dependence was nonlinear during the first heating, but it was perfectly linear during the second heating. By correcting for thermal expansion, the heat-induced relaxation of macrostrain could be obtained. This was done by subtracting the unit cell parameters obtained from the second heating cycle (where the organic material had been removed) from those of the first heating, as shown in Figure 5B.

For *P. carterae*, different behaviors were seen for the *a*- and *c*-axes parameters. At room temperature, the macrostrain was expansive along the *a*-axis but contractive for the *c*-axis. These differences decreased as temperature increased, showing that

DOI: 10.1021/acs.cgd.5b00118
Cryst. Growth Des. 2015, 15, 2761−2767

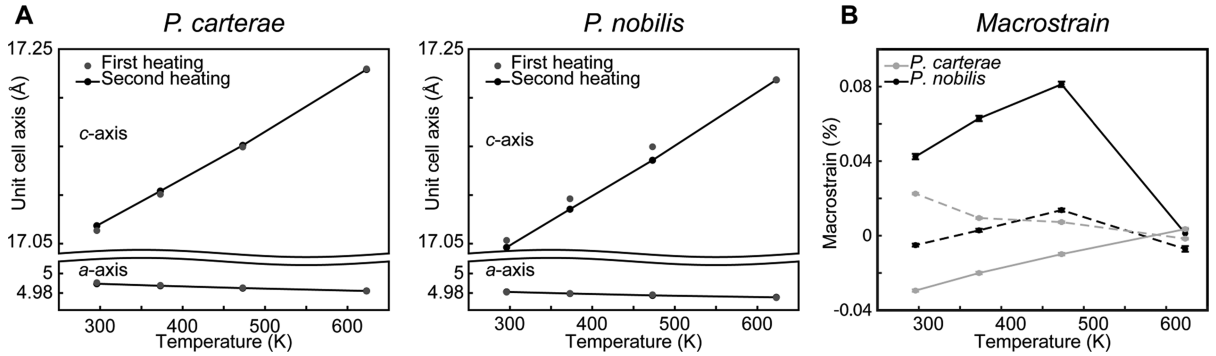

Figure 5. (A) Unit cell *a*- and *c*-axis evolution with temperature for *P. carterae* and *P. nobilis* obtained from Rietveld refinement. Data for the first heating are shown as gray dots, while those from the second heating are shown as connected black dots. (B) Macrostrain calculated as the unit cell parameter in the second cycle subtracted from that of the first cycle and normalized to the room temperature value from the second cycle, i.e., for the *c*-axis at 300 K: $\varepsilon_{300} = (c_{300,1^{st}} - c_{300,2^{nd}})/c_{RT,2^{nd}}\cdot 100\%$. The *a*-axis is indicated by dashed lines. In most cases, standard uncertainties are smaller than the symbol size.

the amount of occluded organic material is an important factor influencing the unit cell size: As the molecules gradually burned off during the first cycle, the difference to the second cycle became smaller.

For *P. nobilis*, the behavior was different. The macrostrain was expansive along *c*, initially increasing with temperature until 623 K, where the organic molecules have burned off and no difference in unit cell size is observed. For the *a*-axis, a behavior similar to the *c*-axis is seen, but with smaller fluctuations starting just below zero macrostrain. This is consistent with trends reported by Pokroy et al.[9] The trends observed for the macrostrain suggests that the organic molecules in the coccoliths and the mollusk shell interact differently with the inorganic phase.

The structural model used in the Rietveld refinements on *P. carterae* included the mean square displacement parameters for each atom, which reflects the combined effects of thermal agitation, static disorder, and possible random systematic error.[56,57] The obtained values are shown as a function of temperature in Figure 6A. In the mean field harmonic approximation, displacement parameters of an atom are described as

$$U_{iso} \approx \frac{\hbar}{2\omega m} \coth\left(\frac{\hbar\omega}{2k_b T}\right) + \delta \quad (1)$$

where ω represents the vibrational frequency and m, the mass of the oscillating atom. $\hbar$ and k_b are constants and T represents temperature. δ is a term independent of temperature which originates from static disorder or systematic error.[56,57] In the classical regime, eq 1 reduces to the linear form:

$$U \approx kT + \delta \quad (2)$$

where k is a constant. Figure 6A also shows fits to such linear expressions. We suggest that the term, δ, is dominated by the effect of occluded biomolecules in the calcite, introducing disorder in the system. For the room temperature data, the difference between the first and second heating cycles thus provides an estimate of $\delta_{organic}$, the disorder contribution from the organic phase, note that the use of the difference also subtracts any common systematic errors such as absorption effects. Values of the differences in atomic displacement parameters between first and second heating cycles, ΔU-iso, are plotted in Figure 6B. As the temperature increases, ΔU-iso decreases because of the gradual burning off of occluded molecules. At 623 K, the differences between the two cycles are within the standard uncertainty, reflecting that the largest part of the biomolecules affecting the mineral has been burned off.

The values of ΔU-iso at room temperature provide an estimate of the disorder introduced into the system by the occluded biomolecules. They are shown for the different types of calcite in Figure 6C. For the fossil calcite in the Klintholm chalk, no significant difference is observed during the heating cycles, whereas for the modern samples, a clear difference after heating is observed.

The values of $\delta_{organic}$ for *P. carterae* differ from those of *P. nobilis*. For the mollusk shell, the largest value is obtained for C followed by Ca and O, whereas for the cultured coccoliths, C has the smallest value and Ca and O are almost the same. The average values for $\delta_{organic}$ for *P. nobilis* and *P. carterae* are 44(17) Å^2 and 21(13) Å^2, i.e., significantly smaller in the coccolith than in the shell. The values of $\delta_{organic}$ reflect the impact of occluded organic molecules on the atoms in the calcite lattice. The large difference in magnitude and order of size for the two modern calcite samples indicates that the atomic scale interactions between the biomolecules and the inorganic phase are different in the two cases.

DISCUSSION AND CONCLUSIONS

The results show that there are significant differences in the effect of occluded biomolecules on the biogenic calcite in mollusk shell and coccolithophores. These differences were reflected in lattice deformation (macrostrain), microstructure (peak widths), and atomic disorder distributions ($\delta_{organic}$). Lattice deformation was also found to be different for aragonite in shells and in the calcified byssus of *Anomia simplex*. This indicates that the details of the biomineralization processes profoundly influence the intimate contact between organic molecules and the inorganic crystals.

The exact mechanism of interaction between functional groups in the organic phase and the forming and growing mineral remains unknown. Many groups have worked on this issue with two approaches dominating: modeling of the interactions between mineral faces organic molecules or the synthesis of calcium carbonates in the presence of additives, either synthetic or extracted from organisms.[19,20,28,42,46,58] Performing true molecular scale experiments is a daunting challenge that, to our knowledge, has not been truly achieved by any researchers on any system. Here, we observe that the

DOI: 10.1021/acs.cgd.5b00118
Cryst. Growth Des. 2015, 15, 2761−2767

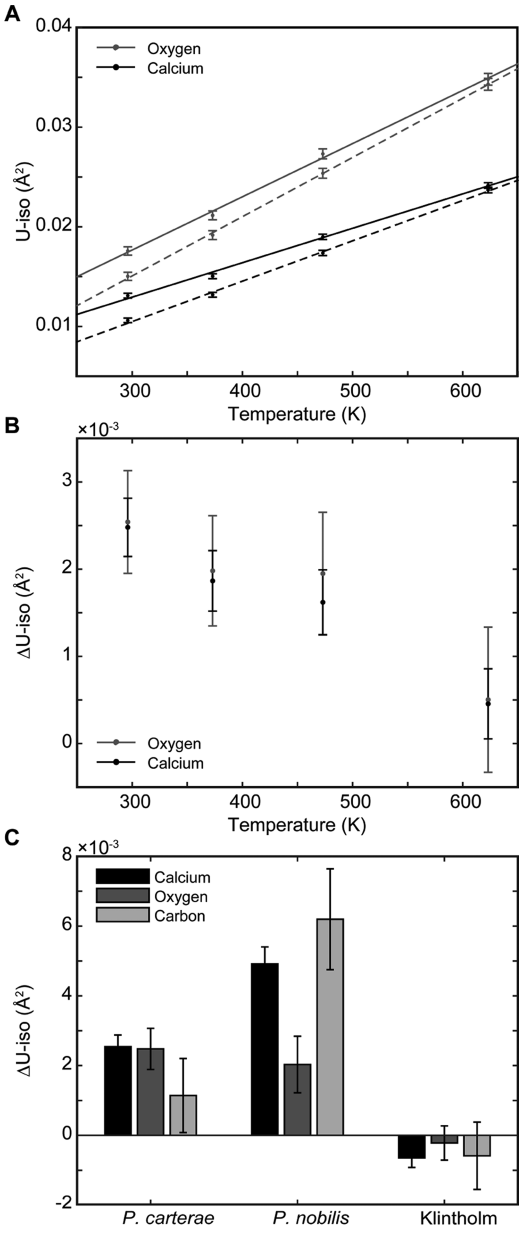

Figure 6. (A) U-iso for oxygen and calcium in calcite for *P. carterae*. Data were obtained with Rietveld refinement and plotted with standard uncertainties as a function of temperature. Lines indicate linear fits expected from classical harmonic vibration; dashed lines are used for the second heating cycle. Carbon resembled calcium so the data were omitted for clarity. (B) ΔU-iso shown as a function of temperature with standard uncertainties. (C) Organic disorder effect, $\delta_{organic}$, estimated as ΔU-iso at room temperature for *P. carterae*, *P. nobilis*, and Klintholm chalk.

magnitude of the effect of occluded biomolecules was consistently smaller in the coccoliths than in the mollusk shell. This suggests that the interaction between biomolecules and calcite is not as tight in the coccoliths as in the shell. This remarkable finding is certainly related to the nature of the interacting macromolecules and functions, acidic aspartic-rich (polyanionic) proteins in the case of *P. nobilis*, and acidic polysaccharides, in the case of the coccolithophore algae. The proteins interacting with biominerals are often very acidic showing how the carboxylic acid moieties interact closely with the mineral phases. In the polysaccharides the presence of sulfate modifications leads to another possible mode of interaction with the mineral, which could be the reason for the differences we observe.

The presence of magnesium in the calcite lattice will induce changes in the absolute value of the unit cell parameters. From the comparison of the unit cell parameters in *P. nobilis* with literature values, we can get a measure of the magnesium content in our samples. However, since the effect of substitution of magnesium in the lattice remains the same after annealing and we report relative changes of lattice parameters, chemical substitution does not affect the present conclusions. In chalk, essentially no impact of occluded biomolecules was observed, and the atomic scale hold of biomolecules on the crystals has thus been released. This is somewhat surprising, given that chalk clearly features recognizable coccolith fragments suggesting that there is a morphology preserving effect and that biomolecules extracted from chalk do influence crystallization of calcite in vitro.[28,29,46] Thus, while the atomic scale influence of biomolecules on crystal lattice and displacement parameters has been released in chalk over the millions of years since its deposition, the overall shape is preserved. For shell, a similar behavior has been observed, where associated biological molecules are partially preserved in fossil samples.[59]

AUTHOR INFORMATION

Corresponding Author

*E-mail: hbirkedal@chem.au.dk.

Notes

The authors declare no competing financial interest.

ACKNOWLEDGMENTS

We acknowledge the European Synchrotron Radiation Facility (ESRF) for provision of synchrotron radiation facilities, and we would like to thank Yves Watier for assistance in using beamline ID31. We thank Dr. Kim N. Dalby for collecting the SEM images and Maria Bjørn for culturing the *P. carterae*. We thank the Danish Council for Independent Research for support for the synchrotron radiation work via DANSCAT as well as funding from the Human Frontiers Science Program, Materials Interface with Biology (MIB) Consortium and the Nano-Chalk Venture. F.M. thanks Sébastien Motreuil (UMR CNRS 6282 Biogéosciences) for sampling *Pinna nobilis* shells and DREAL PACA (Direction Régionale de l'Environnement, de l'Aménagement et du Logement of Provence-Alpes-Côte d'Azur) for delivering the authorization to sample the specimens of *Pinna nobilis* off the marine biology station of Villefranche-sur-Mer.

REFERENCES

(1) Weiner, S.; Addadi, L. *J. Mater. Chem.* **1997**, *7*, 689−702.
(2) Weiner, S.; Dove, P. M. *Rev. Mineral. Geochem.* **2003**, *54*, 1−29.
(3) Mann, S. *Biomineralization: Principles and Concepts in Bioinorganic Materials Chemistry*, 1st ed.; Oxford University Press: New York, 2001; p 198.
(4) Dauphin, Y.; Ball, A. D.; Castillo-Michel, H.; Chevallard, C.; Cuif, J.-P.; Farre, B.; Pouvreau, S.; Salomé, M. *Micron* **2013**, *44*, 373−383.
(5) Okumura, T.; Suzuki, M.; Nagasawa, H.; Kogure, T. *Cryst. Growth Des.* **2011**, *12*, 224−230.
(6) Wegst, U. G. K.; Bai, H.; Saiz, E.; Tomsia, A. P.; Ritchie, R. O. *Nat. Mater.* **2015**, *14*, 23−36.
(7) Pokroy, B.; Fitch, A.; Zolotoyabko, E. *Adv. Mater.* **2006**, *18*, 2363−2368.

DOI: 10.1021/acs.cgd.5b00118
Cryst. Growth Des. 2015, 15, 2761−2767

(8) Pokroy, B.; Quintana, J. P.; Caspi, E. a. N.; Berner, A.; Zolotoyabko, E. *Nat. Mater.* **2004**, *3*, 900−902.
(9) Pokroy, B.; Fitch, A. N.; Marin, F.; Kapon, M.; Adir, N.; Zolotoyabko, E. *J. Struct. Biol.* **2006**, *155*, 96−103.
(10) Pokroy, B.; Fitch, A. N.; Lee, P. L.; Quintana, J. P.; Caspi, E. a. N.; Zolotoyabko, E. *J. Struct. Biol.* **2006**, *153*, 145−150.
(11) Metzger, T. H.; Politi, Y.; Carbone, G.; Bayerlein, B.; Zlotnikov, I.; Zolotoyabko, E.; Fratzl, P. *Cryst. Growth Des.* **2014**, *14*, 5275−5282.
(12) Zolotoyabko, E.; Caspi, E. N.; Fieramosca, J. S.; Von Dreele, R. B.; Marin, F.; Mor, G.; Addadi, L.; Weiner, S.; Politi, Y. *Cryst. Growth Des.* **2010**, *10*, 1207−1214.
(13) Leemreize, H.; Almer, J. D.; Stock, S. R.; Birkedal, H. *J. R. Soc. Interface* **2013**, *10*, 20130319.
(14) Birkedal, H.; Frølich, S.; Leemreize, H.; Stallbohm, R.; Tseng, Y.-H. The Mineralized Byssus of *Anomia simplex:* A Calcified Attachment System. In *Biological and Biomimetic Adhesives Challenges and Opportunities*; Santos, R.; Aldred, N., Gorb, S., Flammang, P., Eds.; RSC Publishing: Cambridge, UK, 2013; pp 16−25.
(15) Eltzholtz, J. R.; Krogsgaard, M.; Birkedal, H. Hierarchical Design and Nanomechanics of the Calcified Byssus of *Anomia simplex*. In *Structure-Property Relationships in Biomineralized and Biomimetic Composites*; Kisailus, D., Estroff, L., Gupta, H. S., Landis, W. J., Zavattieri, P. D., Eds.; Materials Research Society: Warrendale, 2009; Vol. *1187*, pp 83−88.
(16) Eltzholtz, J. R.; Birkedal, H. *J. Adhes.* **2009**, *85*, 590−600.
(17) Leemreize, H.; Eltzholtz, J. R.; Birkedal, H. *Eur. J. Mineral* **2014**, *26*, 517−522.
(18) Lowenstam, H. A.; Weiner, S. *On Biomineralization*, 1st ed.; Oxford University Press: New York, 1989.
(19) Falini, G.; Albeck, S.; Weiner, S.; Addadi, L. *Science* **1996**, *271*, 67−69.
(20) Belcher, A. M.; Wu, X. H.; Christensen, R. J.; Hansma, P. K.; Stucky, G. D.; Morse, D. E. *Nature* **1996**, *381*, 56−58.
(21) Dauphin, Y.; Marin, F. *Experientia* **1995**, *51*, 278−283.
(22) Marxen, J. C.; Hammer, M.; Gehrke, T.; Becker, W. *Biol. Bull. (Woods Hole, MA, U. S.)* **1998**, *194*, 231−240.
(23) Douglas, S. D.; Isenberg, H. D.; Lavine, L. S.; Spicer, S. S. *J. Histochem. Cytochem.* **1967**, *15*, 285−291.
(24) Borman, A. H.; de Jong, E. W.; Huizinga, M.; Kok, D. J.; Westbroek, P.; Bosch, L. *Eur. J. Biochem.* **1982**, *129*, 179−183.
(25) Rao, A.; Berg, J. K.; Kellermeier, M.; Gebauer, D. *Eur. J. Mineral.* **2014**, *26*, 537−552.
(26) Hassenkam, T.; Johnsson, A.; Bechgaard, K.; Stipp, S. L. S. *Proc. Natl. Acad. Sci. U.S.A.* **2011**, *108*, 8571−8576.
(27) Arias, J. L.; Fernández, M. S. *Chem. Rev.* **2008**, *108*, 4475−4482.
(28) Nielsen, J. W.; Sand, K. K.; Pedersen, C. S.; Lakshtanov, L. Z.; Winther, J. R.; Willemoës, M.; Stipp, S. L. S. *Cryst. Growth Des.* **2012**, *12*, 4906−4910.
(29) Sand, K. K.; Pedersen, C. S.; Sjöberg, S.; Nielsen, J. W.; Makovicky, E.; Stipp, S. L. S. *Cryst. Growth Des.* **2014**, *14*, 5486−5494.
(30) Henriksen, K.; Stipp, S. L. S. *Cryst. Growth Des.* **2009**, *9*, 2088−2097.
(31) Young, J. R.; Henriksen, K. *Rev. Mineral. Geochem.* **2003**, *54*, 189−215.
(32) Young, J. R.; Davis, S. A.; Bown, P. R.; Mann, S. *J. Struct. Biol.* **1999**, *126*, 195−215.
(33) Zhang, S.; Gonsalves, K. E. *Langmuir* **1998**, *14*, 6761−6766.
(34) Henriksen, K.; Stipp, S. L. S.; Young, J. R.; Marsh, M. E. *Am. Mineral.* **2004**, *89*, 1709−1716.
(35) Marsh, M. E.; Dickinson, D. P. *Protoplasma* **1997**, *199*, 9−17.
(36) Marsh, M. E. *Protoplasma* **1994**, *177*, 108−122.
(37) Marsh, M. E. Regulation of Coccolith Calcification in *Pleurochrysis carterae*. In *Handbook of Biomineralization*; Wiley-VCH Verlag GmbH: Weinheim, 2008; pp 211−226.
(38) Marsh, M. E. *Protoplasma* **1999**, *207*, 54−66.
(39) Marsh, M. E. Biomineralization in Coccolithophores. In *Biomineralization*; Wiley-VCH Verlag GmbH & Co. KGaA: Weinheim, 2005; pp 195−215.
(40) Marsh, M. E.; Ridall, A. L.; Azadi, P.; Duke, P. J. *J. Struct. Biol.* **2002**, *139*, 39−45.
(41) Dauphin, Y. *J. Biol. Chem.* **2003**, *278*, 15168−15177.
(42) Marin, F.; Amons, R.; Guichard, N.; Stigter, M.; Hecker, A.; Luquet, G.; Layrolle, P.; Alcaraz, G.; Riondet, C.; Westbroek, P. *J. Biol. Chem.* **2005**, *280*, 33895−33908.
(43) Marin, F.; Narayanappa, P.; Motreuil, S. Acidic Shell Proteins of the Mediterranean Fan Mussel *Pinna nobilis*. In *Molecular Biomineralization: Aquatic Organisms Forming Extraordinary Materials - Progress in Molecular and Subcellular Biology, Vol. 52*; Mueller, W. E. G., Ed.; Springer: Berlin, 2011; pp 353−395.
(44) Hassenkam, T.; Skovbjerg, L. L.; Stipp, S. L. S. *Proc. Natl. Acad. Sci. U.S.A.* **2009**, *106*, 6071−6076.
(45) Pedersen, C. S. *Interaction between Reservoir Minerals and Organic Molecules: Implications for Biomineralization and Enhanced Oil Recovery*; University of Copenhagen: Copenhagen, Denmark, 2011.
(46) Yang, M.; Stipp, S. L. S.; Harding, J. *Cryst. Growth Des.* **2008**, *8*, 4066−4074.
(47) Leemreize, H.; Eltzholtz, J. R.; Birkedal, H. *Eur. J. Miner.* **2014**, *26*, 517−522.
(48) Andersson, M. P.; Hem, C. P.; Schultz, L. N.; Nielsen, J. W.; Pedersen, C. S.; Sand, K. K.; Okhrimenko, D. V.; Johnsson, A.; Stipp, S. L. *J. Phys. Chem. A* **2014**, *118*, 10720−9.
(49) Keller, M. D.; Selvin, R. C.; Claus, W.; Guillard, R. R. L. *J. Phycol.* **1987**, *23*, 633−638.
(50) Guillard, R. R. L.; Ryther, J. H. *Can. J. Microbiol.* **1962**, *8*, 229−239.
(51) MATLAB MathWorks, Inc.: Natick, Massachusetts, United States, R2014b.
(52) Post, J. E.; Bish, D. L. Rietveld refinement of crystal structures using powder X-ray diffraction data. In *Reviews in Mineralology and Geochemistry*; Post, J. E., Bish, D. L., Eds.; Mineralogical Society of America: Chantilly, VA, 1989; Vol. *20*, pp 277−308.
(53) Larson, A. C.; Dreele, R. B. V. *General Structure Analysis System (GSAS)*; National Laboratory Report, LAUR 86-748; Los Alamos National Laboratory: Los Alamos, NM, 2004.
(54) Rodriguez-Carvajal, J. *FullProf: A Program for Rietveld Refinement and Pattern Matching Analysis*; Abstracts of the Satellite Meeting on Powder Diffraction of the XV Congress of the IUCr, Toulouse, France, 1990; p 127.
(55) Mackenzie, F. T.; Bischoff, W. D.; Bishop, F. C.; Loijens, M.; Schoonmaker, J.; Wollast, R. *Rev. Mineral. Geochem.* **1983**, *11*, 97−144.
(56) Capelli, S. C.; Bürgi, H. B.; Birkedal, H. *Acta Crystallogr., Sect. A: Found. Crystallogr.* **2000**, *56*, 425−435.
(57) Burgi, H. B.; Capelli, S. C. *Acta Crystallogr., Sect. A: Found. Crystallogr.* **2000**, *56*, 403−412.
(58) Meldrum, F. C.; Cölfen, H. *Chem. Rev.* **2008**, *108*, 4332−4432.
(59) Dauphin, Y.; Denis, A.; Sorel, S. *J. Taph.* **2011**, *9*, 181−200.

DOI: 10.1021/acs.cgd.5b00118
Cryst. Growth Des. 2015, 15, 2761−2767